Installation of Spectrally Selective Imaging System in RF Negative Ion Source

メタデータ	言語: English 出版者: 公開日: 2021-07-13 キーワード (Ja): キーワード (En): 作成者: IKEDA, Katsunori, Wu¨nderlich, D., FANTZ, U., Heinemann, B., KISAKI, Masashi, NAGAOKA, Kenichi, NAKANO, Haruhisa, OSAKABE, Masaki, TSUMORI, Katsuyoshi, Geng, S., KANEKO, Osamu, TAKEIRI, Yasuhiko メールアドレス: 所属:
URL	http://hdl.handle.net/10655/00012576

This work is licensed under a Creative Commons Attribution 3.0 International License.

Installation of Spectrally-selective Imaging System in RF Negative Ion Source[a)]

K. Ikeda,[1, b)] D. Wünderlich,[2] U. Fantz,[2] B. Heinemann,[2] M. Kisaki,[1] K. Nagaoka,[1] H. Nakano,[1] M. Osakabe,[1] K. Tsumori,[1] S. Geng,[3] O. Kaneko,[1] and Y. Takeiri[1]

[1)] *National Institute for Fusion Science, 322-6 Oroshi, Toki, Gifu, 509-5292, Japan*

[2)] *Max-Planck-Institut für Plasmaphysik, Boltzmannstraße 2, 85748 Garching, Germany*

[3)] *The Graduate University for Advanced Studies, 322-6 Oroshi, Toki 509-5292, Japan*

(Dated: 28 September 2015)

A spectrally-selective imaging system has been installed in the RF negative ion source in the ITER-relevant negative ion beam test facility ELISE to investigate distribution of hydrogen Balmer-α emission (H_α) close to the production surface of hydrogen negative ion. We selected a GigE vision camera coupled with an optical band-path filter, which can be controlled remotely using high speed network connection. A distribution of H_α emission near the bias plate has been clearly observed. The same time trend on H_α intensities measured by the imaging diagnostic and the optical emission spectroscopy is confirmed.

PACS numbers: 42.30.-d, 41.75.Cn

I. INTRODUCTION

A spectrally-selective imaging system has been developed and installed in the arc discharge type negative hydrogen ion (H^-) source in the National Institute for Fusion Science (NIFS).[1,2] This system has performed well for visualizing a reduction in the distribution of hydrogen Balmer-α emission (H_α) owing to H^- ions. These findings have contributed to the high performance and safety operation for a neutral beam injector (NBI) in the Large Helical Device (LHD).

On the other hand, large scale H^- source based on RF discharge will be constructed for the NBI at the International Thermonuclear Experimental Reactor (ITER).[3] Optimization of RF source performance and variable operation outputs have been carried out from a half-size H^- source in the ELISE test facility at Max-Planck-Institut für Plasmaphysik (IPP) Garching.[4] Current densities near the ITER NBI requirements have been achieved in hydrogen with low co-extracted electrons.[5] An optical emission spectroscopy (OES) diagnostic is kept running in the ELISE operation to obtain plasma parameters and its homogeneity.[6] Distribution of H_α has a capability to obtain extraction behavior of electrons and negative hydrogen ions in H^- source[1,2,7] , which is also important knowledge for production of high power beam and optimization of beam shape.

In this paper, we present a configuration of a spectrally-selective imaging system based on a GigE vision camera for the ELISE RF hydrogen negative ion source. A clear high-resolution monochromatic image has been taken, and a value of distance per pixel of image is obtained by scale calibration. We will show the distribution image of H_α emission close to the bias plate surface in the typical RF discharge.

II. CONFIGURATION OF SPECTRALLY-SELECTIVE IMAGING SYSTEM

Figure 1 shows the schematic drawing of the RF hydrogen negative ion source in ELISE. Hydrogen plasmas are generated in four cylindrical RF drivers by six-turn copper coils, and the plasmas expand into the extraction region near a plasma grid (PG) surface. A metal bias plate (BP) with eight opening windows around the beamlet groups covers the PG surface. Hydrogen negative ions are produced on cesiated metal surfaces and are extracted through the apertures. The 28 diagnostic ports (14 in horizontal and 14 in vertical) are positioned in the source at the upstream position for observing near the BP surface.[6] We set a spectrally-selective imaging system at the XR−1U port with the diameter of 40 mm quartz window. The line of sight (LOS) is arranged paralleled to the BP and PG surface with the distance of 7 mm and 20 mm, respectively, from the port center. The LOS traverse the groups of the extraction apertures, which is advantage to observe the change in optical signal owing to beam extraction. The opposite side viewing port of XL−1U is used for optical emission spectroscopy (OES) to observe time trace of H_α, H_β, H_γ, and Cs spectrum in the source. We use a survey spectrometer (PLASUS : EMICON MC system) with the wavelength range of 180 $\sim$ 880 nm and sampling rate $<$ 15 Hz[6].

Figure 2 shows the system configuration of the spectrally-selective imaging system. We use a network

---

[a)] Contributed paper, published as part of the Proceedings of the 16th International Conference on Ion Sources, New York City, NY, August, 2015

[b)] ikeda.katsunori@lhd.nifs.ac.jp

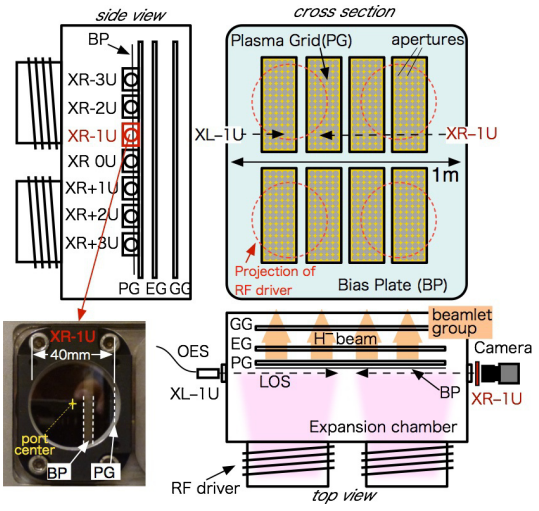

FIG. 1. Schematic cross-section drawing of RF hydrogen negative ion source for ELISE. The LOS for imaging diagnostic located on the XR−1U port is across extraction region near the BP surface. The OES diagnostics are set on the opposite side of the viewing ports XL−1U.

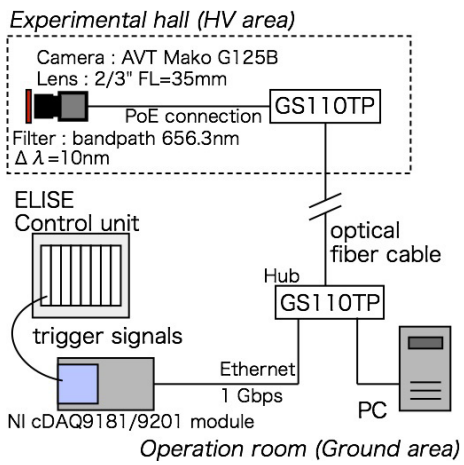

FIG. 2. Schematic diagram of the spectrally-selective imaging system. The CCD camera is mounted on the H^- source of high-voltage state in the experimental hall for ELISE. That is controlled in the operation room using a fast Ethernet network connection. Trigger signals are acquired by a compact DAQ system connected to the same network.

connection CCD camera (AVT : MAKO G125B) based on the GigE vision standard. The type of charge-coupled device (CCD) detector (Sony : ICX445ALA) is a progressive black and white sensor which size is 1/3 inch. The effective chip size is 4.8 mm × 3.6 mm with the pixel resolution of 1292 × 964 pixels using a square cell of 3.75 μm. We use a 2/3 inch C-mount lens with focal length of 35 mm; the focal point is fixed 52 cm away from the lens, which is the center of the ion source. An interference band path filter for H_α emission with the central wave length of 656.3 nm and 10 nm full width half maximum (FWHM) is inserted in front of the lens. The camera is driven by 12 V DC power suppled from a PoE (Power on Ethernet) hub (NETGEAR: GS110TP) located on a high voltage rack in the experimental hall. The CCD camera is remotely controlled from the operation room for ELISE using the fast internal Ethernet network with optical fibers. The image in 12-bit monochrome is captured at the timing of the trigger signal detected by a compact DAQ system (NI: cDAQ9181 with 9201 module) connected with the same network.

III. SPATIAL SCALE CALIBRATION AND DISTRIBUTION OF H_α EMISSION

We set up a scale sheet in front of the CCD camera before installation on ELISE. The distance of the scale sheet and the CCD camera is 52 cm, which is equivalent to the center position of the ion source. Figure 3(a) shows the scale sheet image; focus condition and optical distortion is good enough to obtain a distribution. We obtain the coordinate of the points of intersection of the vertical and horizontal lines, and confirm the proportional relationship of pixel number and distance as shown in Figure 3(b). The spatial distance per pixel corresponds to 0.055 mm/pixel at the center of the source.

Figure 4(a) shows a typical output image for the wavelength of 656 nm taken by the spectrally-selective imaging system with 40 ms exposure time in hydrogen RF discharge at the shot number of 8788 in ELISE. The discharge power and filling gas pressure is 40 kW per driver and 0.6 Pa, respectively. Discharge area is located 300 mm left from the LOS center, which is outside of the image. The surface facing the CCD camera inside the source is illuminated by the reflected light from the hydrogen plasma, but the circle area where there is a hollow place on the opposite side viewing port becomes dark. The BP surface is located on the right side of the image between 850 and 1080 pixels; opening windows cutting in the BP around the beamlet groups look like narrow slits. We superimpose the dotted circles for the angle θ from the center of LOS (θ = 2°, 3°, and 4°). Viewing angle of θ = 4° covers the area 35 mm away from the LOS center. The central wavelength (λ_0) of the interference band-path filter changes 0.5 nm at the incident angle of 4°. Distribution measurement is not affected by incident angle because this change is small compared to the 10 nm FWHM.

Figure 4(b) shows the horizontal distribution of H_α emission through the center of LOS for imaging diagnostic. Horizontal axis is the distance from the position of OES port, which is converted by the value for spatial distance per pixel. We find sharp signal increase at the boundary of viewing port due to increase of reflection signal from the inner surface. The signal contribution of reflection is 17%. The signal intensity of H_α emission gradually increases in the upstream direction (left side). We expect this distribution relate with a distribution of hydrogen ions and electrons. Figure 4(c) shows the time

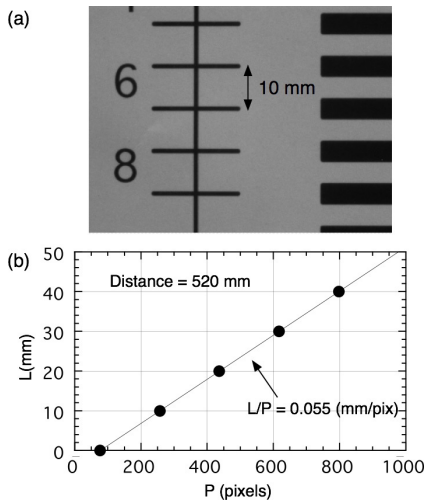

FIG. 3. (a) A detected image of scale arranged at 52 cm in front of the CCD camera. (b) Comparison of a pixel number and scale, a solid line is the fitting line by linear function.

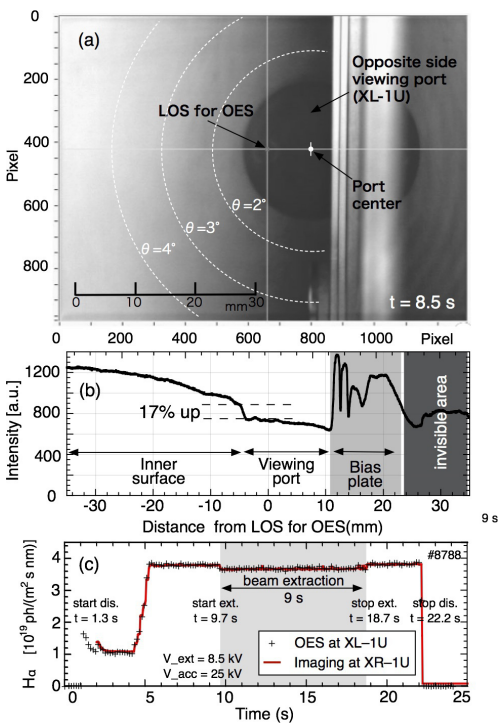

FIG. 4. (a) Photographic image for RF discharge taken by the imaging system at the XR−1U. (b)Horizontal distribution of H_α emission through the center of LOS. (c) Time traces of H_α intensity measured by the OES and imaging diagnostic at the same position.

traces of H_α intensity measured by OES and imaging diagnostic at XL−1U and XR−1U, respectively. Time trend of the signal intensity of imaging measurement is in good agreement with the OES signal. Therefore, the comparison with calibrated OES signal is helpful to estimate the intensity distribution of H_α emission taken by imaging system. We find sudden signal reduction on H_α emission during beam extraction in both measurements. The cause of this reduction is not clear at present with regard to whether the main contribution is decrease of electrons or H^- ions in this discharge. To review details of its reduction on imaging diagnostic, a density measurement of negative ions and electrons will be needed at the same places and the same discharge.

IV. CONCLUSION

A spectrally-selective imaging system has performed well in the RF negative ion source in the ITER-relevant negative ion beam test facility ELISE. A distribution of H_α reductions are clearly observed. The time trend intensity is consistent with the H_α intensity measured by OES at the same position. Therefore, signal intensity of the image can be calibrated by calibrated OES measurement. The future direction of this study will be an identification of the relationship between an H_α emission intensity and an H^- density, that will contribute to optimize RF source performance for ELISE and ITER-NBI.

ACKNOWLEDGMENTS

We are grateful to the late Dr. P. Franzen whose support and useful discussions were extremely valuable throughout this study. We also thank technical staff at IPP Garching for arrangement of diagnostic and ELISE operation. The authors acknowledge the financial support by SOKENDAI Young Researchers Overseas Visit Program to conduct research at IPP Garching. This research is also supported by JSPS KAKENHI Grant Number 25249134, and the budget for the NIFS No. ULRR702 and No. ULRR009.

[1] K. Ikeda, H. Nakano, K. Tsumori, M. Kisaki, K. Nagaoka, M. Osakabe, Y. Takeiri, and O. Kaneko, New J. Phys. **15**, 1367 (2013).
[2] K. Ikeda, H. Nakano, K. Tsumori, M. Kisaki, K. Nagaoka, M. Osakabe, Y. Takeiri, and O. Kaneko, Rev. Sci. Instrum. **85**, 02A724 (2014).
[3] R. Hemsworth, H. Decamps, J. Graceffa, B. Schunke, M. Tanaka, M. Dremel, A. Tanga, H. D. Esch, F. Geli, J. Milnes, T. Inoue, D. Marcuzzi, P. Sonato, and P. Zaccaria, Nucl. Fusion **49**, 045006 (2009).
[4] B. Heinemann, H. D. Falter, U. Fantz, P. Franzen, M. Froeschle, W. Kraus, C. Martens, R. Nocentini, R. Riedl, E. Speth, and A. Staebler, Fusion Eng. Des. **86**, 768 (2011).
[5] P. Franzen, D. Wünderlich, R. Riedl, R. Nocentini, F. Bonomo, U. Fantz, M. Fröschle, B. Heinemann, C. Martens, W. Kraus, A. Pimazzoni, and B. Ruf, AIP Conf. Proc. **1655**, 060001 (2015).
[6] D. Wünderlich, U. Fantz, P. Franzen, R. Riedl, and F. Bonomo, Rev. Sci. Instrum. **84**, 093102 (2013).
[7] U. Fantz, H. Falter, P. Franzen, D. Wünderlich, M. Berger, A. Lorenz, W. Kraus, P. McNeely, R. Riedl, and E. Speth, Nucl. Fusion **46**, S297 (2006).